

Character decomposition of Potts model partition functions.

I. Cyclic geometry

Jean-François Richard^{1,2} and Jesper Lykke Jacobsen^{1,3}

¹*Laboratoire de Physique Théorique et Modèles Statistiques
Université Paris-Sud, Bât. 100, 91405 Orsay, France*

²*Laboratoire de Physique Théorique et Hautes Energies
Université Paris VI, Boîte 126, Tour 24, 5^{ème} étage
4 place Jussieu, 75252 Paris cedex 05, France*

³*Service de Physique Théorique
CEA Saclay, Orme des Merisiers, 91191 Gif-sur-Yvette, France*

February 4, 2008

Abstract

We study the Potts model (defined geometrically in the cluster picture) on finite two-dimensional lattices of size $L \times N$, with boundary conditions that are free in the L -direction and periodic in the N -direction. The decomposition of the partition function in terms of the characters K_{1+2l} (with $l = 0, 1, \dots, L$) has previously been studied using various approaches (quantum groups, combinatorics, transfer matrices). We first show that the K_{1+2l} thus defined actually coincide, and can be written as traces of suitable transfer matrices in the cluster picture. We then proceed to similarly decompose constrained partition functions in which exactly j clusters are non-contractible with respect to the periodic lattice direction, and a partition function with fixed transverse boundary conditions.

1 Introduction

The Q -state Potts model on a graph $G = (V, E)$ is defined initially for Q integer by the partition function

$$Z = \sum_{\{\sigma\}} \exp \left[J \sum_{(i,j) \in E} \delta(\sigma_i, \sigma_j) \right], \quad (1)$$

where the spins $\sigma_i = 1, 2, \dots, Q$ live on the vertices V , and the interaction of strength J is along the edges E . This definition can be extended to arbitrary real values of Q through the high-temperature expansion of Z , yielding [1]

$$Z = \sum_{E' \subseteq E} Q^{n(E')} (e^J - 1)^{b(E')}, \quad (2)$$

where $n(E')$ and $b(E') = |E'|$ are respectively the number of connected components (clusters) and the cardinality (number of links) of the edge subsets E' .

It is standard to introduce the temperature parameters $v = e^J - 1$ and $x = Q^{-1/2}v$, and to parametrize the interval $Q \in [0, 4)$ by $Q^{1/2} = 2 \cos(\pi/p) = q + q^{-1}$ with $p \geq 2$ and $q = \exp(i\pi/p)$.

In two dimensions, much knowledge about the continuum-limit behaviour of the Potts model has accumulated over the years, thanks mainly to the progress made in conformal field theory and the theory of integrable systems. This is particularly true at the ferromagnetic critical point, whereas much work remains to be done in the more difficult antiferromagnetic regime.

In this paper, we shall take a different point of view, and consider a number of combinatorial results which hold exactly true on arbitrary regular lattices of any finite size $L \times N$, and at any temperature x . The choice of boundary conditions is clearly important. In the following we shall consider the *cyclic* case (free boundary conditions in the L -direction and periodic in the N -direction), and relegate the more complicated *toroidal* case (periodic boundary conditions in both directions) to a companion paper [2].

For simplicity we denote henceforth V the number of vertices, E the total number of edges, and F the number of faces, including the exterior one. Also, we often consider the lattice as being built up by a transfer matrix T propagating in the N -direction, which we represent as horizontal.

The case of cyclic boundary conditions has already been considered by Pasquier and Saleur [3], where it was shown how to decompose Z as a linear combination of characters $K_{1,2l+1}$ (with $l = 0, 1, \dots, L$) of representations of the quantum group $U_q(sl(2))$. Further developments were made independently in [4, 5]. Chang and Shrock [4] recovered the same decomposition, but with $K_{1,2l+1}$ defined as a partial trace of the transfer matrix T_{spin} in the spin representation. Jacobsen and Salas [5] used a similar decomposition, but with $K_{1,2l+1}$ defined as a matrix element of a transfer matrix in the cluster representation involving two time-slices. We show here that all three points of view are in fact equivalent, and that the characters $K_{1,2l+1}$ obtained are identical.

Apart from that, the main part of our discussion is in the cluster picture, following [5]. We recall the relevant definitions in section 2.

The cluster configurations contributing to $K_{1,2l+1}$ turn out to be those in which $j \geq l$ clusters are non-contractible with respect to the periodic lattice direction. We henceforth refer to such clusters as *non-trivial clusters*, or NTC for brevity. In section 3 we give the character decomposition of constrained partition functions Z_{2j+1} in which the number of NTC is precisely j . This gives as a by-product the character decomposition of the full partition function Z , in agreement with [3, 4].

Finally, we obtain in section 4 the character decomposition of a partition function with *fixed* (rather than free) transverse boundary conditions. The physical implications of our results are discussed in section 5.

2 Cluster representation of the Potts model

2.1 Transfer matrix in the cluster representation

The cluster representation of the Potts model is defined by Eq. (2). Since the clusters are non-local objects, it is not a priori obvious how to build the partition function using a transfer matrix. The key to tackle the problem of non-locality is to introduce a basis of states that takes into account connectivity information [6]. However, the periodic boundary conditions in the longitudinal direction introduces a further complication, whose resolution necessitates to introduce a transfer matrix that acts between *two* time

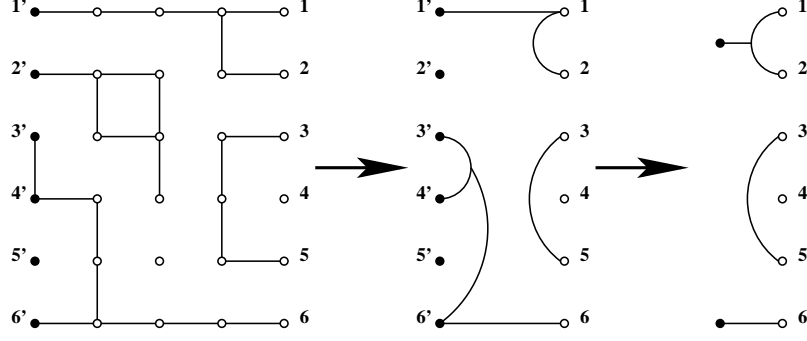


Figure 1: Example of a cluster configuration on a part of the square lattice with width $L = 6$ (left part) and the corresponding connectivity state involving two time slices (middle part). The points in the right (resp. left) time slice are represented as white (resp. black) circles and are labelled $1, 2, \dots, L$ (resp. $1', 2', \dots, L'$). The corresponding partition is $|v_P\rangle = (1'12)(2')(3'4'6'6)(5')(35)(4)$. There are two bridges, i.e., independent connections between the left and right time slices. With the number of bridges given, the transfer matrix elements are independent of the connectivity information on the left time slice. This fact can be expressed graphically by assigning to each bridge an unlabelled black point and depicting the right time slice only (right part of the figure).

slices [5].

We therefore begin by reviewing how to write the transfer matrix T in the cluster representation when the boundary conditions are cyclic [5]. The relevant geometry is shown in the left part of Fig. 1.¹ Unlike the case of free boundary conditions in the longitudinal direction, one must take care not only of the connectivities inside the right time slice (at time $t = t_0$), i.e., between the points labelled $\{1, 2, \dots, L\}$, but also of the connectivities of the left time slice (at time $t = 0$), i.e., between the points $\{1', 2', \dots, L'\}$, and of the connectivities linking the two time slices. The transfer matrix propagates the right time slice from time t_0 to time $t_0 + 1$. Therefore, the space on which the transfer matrix acts is the space of connectivity patterns $|v_P\rangle$ associated to partitions of the set $\{1', \dots, L', L, \dots, 1\}$. Because of the planarity of the lattice only non-crossing partitions are allowed. An example of an allowed partition and its graphical representation is shown

¹Here, and in all subsequent figures, the explicit examples of configurations are for the geometry of the square lattice. We however stress that our reasoning is quite general and applies to an arbitrary lattice which is weakly regular, in the sense that the number of points in each time slice is equal to L .

in the middle part of Fig. 1.

A formal expression of the transfer matrix is given in [5]. Here we just give the practical rules to calculate its elements. As in the case of free longitudinal boundary conditions, there is a weight v per coloured link and a weight Q per cluster [see Eq. (2)], except for the clusters containing a black circle which have a weight equal to 1. Of particular interest are the components of a partition that contain both white and black circles. Such components are called bridges; we denote by l the total number of bridges in the partition (in Fig. 1, $l = 2$). When at a time t , i.e., after applying t times the transfer matrix, one obtains a state with l bridges, it means that there are l clusters which begin at $t = 0$ and end at a time $\geq t$. Note that the initial connectivity (at $t = 0$) is the unique state with L bridges, meaning that the left and right time slices coincide. Denoting this state $|v_L\rangle$, the partition function Z is given by

$$Z = \langle u | T^N | v_L \rangle, \quad (3)$$

where $\langle u |$ takes into account the periodic longitudinal boundary conditions, by re-identifying the left and right time slices at time $t = N$ and assigning a weight Q to each of the resulting clusters [5].

Two important observations must be made:

1. T propagates the right time slice, and so, cannot modify the connectivity inside the left time slice.
2. Under the action of T , the number of bridges l can only decrease or stay constant.

These two properties imply that the transfer matrix has a lower-triangular block form:

$$T = \begin{pmatrix} T_{L,L} & 0 & \dots & 0 \\ T_{L-1,L} & T_{L-1,L-1} & \dots & 0 \\ \vdots & \vdots & & \vdots \\ T_{0,L} & T_{0,L-1} & \dots & T_{0,0} \end{pmatrix} \quad (4)$$

Furthermore, they also imply that each block $T_{l,l}$ on the diagonal of T has itself a diagonal

block form:

$$T_{l,l} = \begin{pmatrix} T_{l,l}^{(1)} & 0 & \dots & 0 \\ 0 & T_{l,l}^{(2)} & \dots & 0 \\ \vdots & \vdots & & \vdots \\ 0 & 0 & \dots & T_{l,l}^{(N_l)} \end{pmatrix} \quad (5)$$

Each sub-block $T_{l,l}^{(j)}$ is characterized by a certain left slice connectivity and a position of the l bridges. Its dimension is given by the number of compatible right slice connectivities. In fact, the N_l sub-blocks $T_{l,l}^{(j)}$, with $1 \leq j \leq N_l$, are exactly equal, as the rules for computing their matrix elements coincide. Indeed, the L white circles of the right slice do not “see” the left slice connectivity and from where the l bridges emanate; only the number l of bridges matters. In particular, the dimension $n(L, l)$ of the sub-block $T_{l,l}^{(j)}$ is independent of j . Moreover, because of the symmetry between the left and right time slices, the number of sub-blocks equals their dimension, $N_l = n(L, l)$. It can be proved that [3, 4]:

$$n(L, l) = \frac{2l+1}{L+l+1} \binom{2L}{L-l} = \binom{2L}{L-l} - \binom{2L}{L-l-1}. \quad (6)$$

Note that $n(L, 0) = C_L$, the L 'th Catalan number, which is the dimension of the cluster transfer matrix with *free* longitudinal boundary conditions. Indeed, each sub-block $T_{0,0}^{(j)}$ is equal to the usual single time slice cluster transfer matrix [6].²

Because of the block structure of T , its eigenvalues are the union of the eigenvalues of the sub-blocks $T_{l,l}^{(j)}$. Therefore, the sub-blocks with given l being equal, one can obtain all the eigenvalues of T by considering only one reference sub-block for each given number of bridges l [5]. For instance, one can choose as reference sub-block the one

²Note that the last part of these results differ from those given in [5]. Namely, the authors of [5] studied the chromatic polynomial ($v = -1$), so the connectivities between neighbouring points were forbidden, and therefore the dimension of each sub-block was smaller than $n(l, L)$ given by Eq. (6). Furthermore, in the case of a square lattice, the authors symmetrized T with respect to a top-bottom reflection of the strip. This not only diminishes the total dimension of the transfer matrix, but also the number of sub-blocks. At the same time it makes the structure of T slightly more complicated. Indeed, there would then be two types of sub-blocks, depending on whether the left slice connectivity and the position of the l bridges are symmetric or non-symmetric with respect to the reflection. The symmetrization couples either pairs of non-symmetric sub-blocks, or pairs of states inside a symmetric sub-block. Therefore, the symmetric and non-symmetric sub-blocks have different dimensions, the non-symmetric sub-blocks having the largest dimension $n(L, l)$.

with no connection between black circles and with l bridges beginning at $\{1', 2', \dots, l'\}$. Alternatively, one may forget the labelling of the left time slice altogether, and simply mark by a black point each of the components of the right-slice connectivity which form part of a bridge.³ This latter choice is represented in the right part of Fig. 1. In the following, we denote the reference sub-block simply T_l .

2.2 Definition of the characters $K_{1,2l+1}$

It follows from Eq. (3) and the preceding discussion that

$$Z = \sum_{l=0}^L \sum_{i=1}^{n(L,l)} c(L, l, i, x) [\lambda_{l,i}(L, x)]^N, \quad (7)$$

where a priori the amplitudes c of the eigenvalues $\lambda_{l,i}(L, x)$ (i labels the distinct eigenvalues within the sub-block T_l) depend of the width L , the number of bridges l , the label i , and the temperature x . In fact, it has been proved in [3, 4], and used in [5], that c depend only of l (and the value of Q chosen). We therefore denote them $c^{(l)}$ in the following. Thus,

$$Z = \sum_{l=0}^L c^{(l)} K_{1,2l+1}(L, N, x), \quad (8)$$

where the $K_{1,2l+1}(L, N, x)$ are defined as

$$K_{1,2l+1}(L, N, x) = \sum_{i=1}^{n(L,l)} [\lambda_{l,i}(L, x)]^N. \quad (9)$$

$K_{1,2l+1}$ is thus simply equal to $\text{Tr}(T_l)^N$.

The notation $K_{1,2l+1}$ (instead of just K_l) is motivated by the fact that at the ferromagnetic critical point ($x_c = 1$ for the square lattice), and in the continuum limit, these quantities become special cases of a generic character $K_{r,s}$ of conformal field theory (CFT) [3]. More precisely, the character $K_{r,s}$ corresponds to the holomorphic dimension $h_{1,2l+1}$ of the CFT with central charge $c = 1 - \frac{6}{p(p-1)}$. For generic (irrational) values of p this CFT is non-unitary and non-minimal. We shall comment on the case of p integer later, in section 3.4. We stress that we have here defined $K_{1,2l+1}$ combinatorially for an

³Note that this choice must respect planarity: only the unnested connectivity components (i.e., those accessible from the far left) can be marked by a black point.

$L \times N$ system, at any temperature x , with no continuum limit being taken; we shall nevertheless refer to them as characters.

The amplitudes $c^{(l)}$ appearing in Eq. (8) are q -deformed numbers [3, 4]

$$c^{(l)} = (2l + 1)_q = \frac{\sin(\pi(2l + 1)/p)}{\sin(\pi/p)} = \sum_{j=0}^l (-1)^{l-j} \binom{l+j}{l-j} Q^j. \quad (10)$$

Note that $c^{(l)}$ is a polynomial of degree l in Q . In the next section, we obtain a new proof of Eq. (10), as a by-product of a more general result in which we give a combinatorial sense to each term in the polynomial separately.

In the remainder of the article, we shall decompose various partition functions as linear combinations of the characters $K_{1,2l+1}$. Indeed, the $K_{1,2l+1}$ are simply related to the eigenvalues of the transfer matrix and can be considered as the basis building blocks of various restricted partition functions.

2.3 Equivalence with Chang and Shrock

We now show that the $K_{1,2l+1}$, that we have defined above following [5], coincide with the partial traces defined in [4].

In [4], Chang and Shrock considered the Potts model partition function in the spin representation: writing $Z = \text{Tr}(T_{\text{spin}})^N$ they decomposed the spin space as a direct sum of what they called level l subspaces. By definition, the level l subspace corresponds to the space generated by applying T_{spin} to the sum of spin states with l spins fixed to l given values. The restriction of T_{spin} to the level l subspace is exactly equal to our matrix T_l (with l connectivity components marked by black points), as they have the same calculation rules (marking a cluster with a black point corresponds to fixing its spin state, i.e., to giving it a weight 1 instead of Q) and a very similar graphical representation of the states (resembling the right part of Fig. 1). The character $K_{1,2l+1}$ appears therefore in [5] as the restriction of the trace to the level l subspace.

We remark that the physical interpretation of the amplitudes $c^{(l)}$ made in [4] is somewhat different from ours. Indeed, at level l Chang and Shrock considered all the independent possibilities of attributing values to l fixed spins, taking into account that some of those possibilities were already present at lower levels. Accordingly, they interpreted

$c^{(l)}$ as the number of level l states independent among themselves, and independent of states at lower levels, and computed $c^{(l)}$ diagrammatically.

Proving the equivalence of our $K_{1,2l+1}$ with those of Pasquier and Saleur requires some further background material, and is deferred to section 3.3.

3 Partition function with a fixed number of non-trivial clusters

In this section we study the character decomposition of constrained partition functions Z_{2j+1} in which the number of non-trivial clusters (NTC) is fixed to j , for $j = 0, 1, \dots, L$. It is important to notice that this is different from the characters $K_{1,2l+1}$, which are related to blocks of the transfer matrix with l bridges.⁴ When imposing the periodic longitudinal boundary conditions, each bridge becomes essentially a *marked* NTC. Since $K_{1,2l+1}$ may contain further NTC which are not marked, we expect $K_{1,2l+1}$ to be a linear combination of several Z_{2j+1} with $j \geq l$. Conversely, since upon acting with the transfer matrix the number of bridges can only decrease or stay constant, we also expect Z_{2j+1} to be a linear combination of several $K_{1,2l+1}$ with $l \geq j$.

The primary goal of this section is to obtain the character decomposition of Z_{2j+1} . In the following two subsections we therefore first express the $K_{1,2l+1}$ in terms of the Z_{2j+1} , and then invert the resulting relations.

3.1 $K_{1,2l+1}$ in terms of Z_{2j+1}

Recalling that $K_{1,2l+1} = \text{Tr} (T_l)^N$, we can write

$$K_{1,2l+1} = \sum_{i=1}^{n(L,l)} \langle v_{l,i} | T^N | v_{l,i} \rangle, \quad (11)$$

where the $|v_{l,i}\rangle$ are the $n(L, l)$ possible connectivity states with l bridges, i.e., states such as those shown in the right part of Fig. 1 with l black points.

⁴To avoid confusion, j will from now on always denote the number of NTC in Z_{2j+1} , and l will denote the number of bridges in $K_{1,2l+1}$.

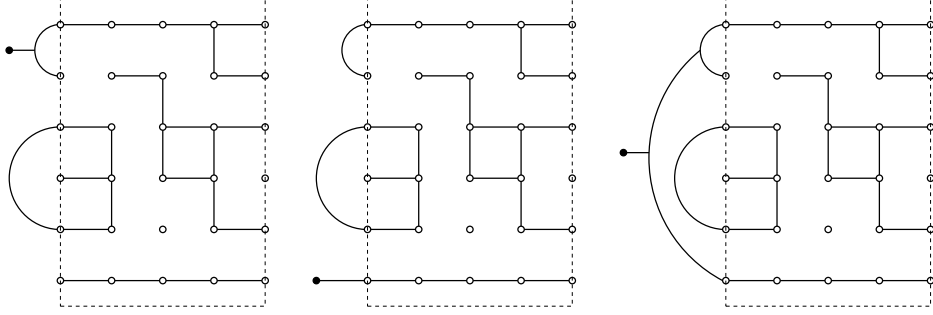


Figure 2: A cluster configuration on a portion of the square lattice (shown inside a dashed box for clarity) and the three compatible connectivity states (shown on the left of each copy of the cluster configuration). In each of the three cases, the final connectivity (i.e., the way in which the L points on the rightmost column of the lattice are interconnected and marked by black points through the cluster configuration *and* the connectivity state on the left) is equal to the initial connectivity state.

We first show that a given cluster configuration with j NTC is contained $n(j, l)$ times in $K_{1, 2l+1}$. To this end, we define that a connectivity state $|v_{l,i}\rangle$ is *compatible* with a given cluster configuration if the action of the cluster configuration on $|v_{l,i}\rangle$ (in the sense of a transfer matrix acting towards the right) yields the same connectivity $|v_{l,i}\rangle$. An example is shown in Fig. 2. It is useful to “forget” for a moment that the longitudinal boundary conditions are cyclic, i.e., to consider the leftmost and rightmost columns of the lattice as distinct. Indeed, the periodic boundary conditions are already encoded in the fact that the final and initial states in Eq. (11) must coincide. The goal is then to show that any cluster configuration with j NTC is compatible with precisely $n(j, l)$ different connectivity states.

Consider then a given cluster configuration with j NTC, with the k 'th NTC ($k = 1, 2, \dots, j$) connecting onto the points $\{y_k\}$ of the rightmost column. For example, in Fig. 2 we have $\{y_1\} = \{1, 2\}$ and $\{y_2\} = \{6\}$. The connectivity states $|v_{l,i}\rangle$ compatible with the cluster configuration can be constructed as follows:

1. The connectivities of the points $y \notin \cup_{k=1}^j \{y_k\}$ must be connected in the same way in $|v_{l,i}\rangle$ as in the cluster configuration. For instance, in Fig. 2 the points $y = 3, 5$ must be connected.
2. The points $\{y_k\}$ within the same bridge (for example, $y = 1, 2$ in Fig. 2) must be

connected in $|v_{l,i}\rangle$.

3. One can independently choose to associate or not a black point to each of the sets $\{y_k\}$. One is free to connect or not two distinct sets $\{y_k\}$ and $\{y_{k'}\}$.

Clearly, the rules 1 and 2 leave no choice. The rule 3 implies in particular that $j \geq l$, or else there is no compatible state $|v_{l,i}\rangle$. The choices mentioned in rule 3 then leave us $n(j, l)$ possibilities for constructing a compatible $|v_{l,i}\rangle$.

We have therefore shown that a given cluster configuration with j NTC is contained $n(j, l)$ times in $K_{1,2l+1}$. As $K_{1,2l+1}$ is simply a trace, each of its NTC carries a weight of 1, whereas the j NTC in Z_{2j+1} each have the usual cluster weight of Q . We therefore arrive at the result

$$K_{1,2l+1} = \sum_{j=l}^L n(j, l) \frac{Z_{2j+1}}{Q^j} \quad (12)$$

where we recall that $n(j, l)$ has been defined in Eq. (6).

3.2 Z_{2j+1} in terms of $K_{1,2l+1}$

Inverting the relations (12) yields

$$Z_{2j+1} = \sum_{l=j}^L c_j^{(l)} K_{1,2l+1} \quad (13)$$

with the coefficients $c_j^{(l)}$ given by

$$c_j^{(l)} = (-1)^{l-j} \binom{l+j}{l-j} Q^j. \quad (14)$$

An interesting special case, which we will refer to in the following, is obtained for $j = 0$, i.e., by disallowing any NTC. From Eqs. (13)–(14), we obtain an alternating sum of the $K_{1,2l+1}$:

$$Z_1 = \sum_{l=0}^L (-1)^l K_{1,2l+1} \quad (15)$$

Note also that the total partition function of the Potts model is given by

$$Z = \sum_{j=0}^L Z_{2j+1}. \quad (16)$$

Comparing Eqs. (14) and (10) we infer that

$$c^{(l)} = \sum_{j=0}^l c_j^{(l)} \quad (17)$$

and from Eqs. (13) and (16) we obtain as promised Eq. (8) for the full partition function.

Interestingly, then, the effect of fixing the number of NTC to j is to keep only the term multiplying Q^j in the expression (10) of $c^{(l)}$. As $c^{(l)}$ is polynomial of degree l in Q , only the $K_{1,2l+1}$ with $l \geq j$ contribute to the character decomposition of Z_{2j+1} . This is in agreement with the physical argument given at the beginning of section 3.

3.3 Equivalence with Pasquier and Saleur

We can now prove that the $K_{1,2l+1}$ defined in [3] using the six-vertex model are equal to the $K_{1,2l+1}$ we defined in Eq. (9) using the cluster transfer matrix. Before attacking the proof, let us briefly recall where the connection with the six-vertex model comes from.

On a planar lattice, the cluster representation of the Potts model partition function is equivalent to a loop representation, where the loops are defined on the medial lattice and surround the clusters [7]. From Eq. (2) and the Euler relation, the weight of a loop configuration E' is $Q^{(V+c(E'))/2} x^{b(E')}$, where $c(E')$ is its number of loops.⁵ An oriented loop representation is obtained by independently assigning an orientation to each loop, with weight q (resp. q^{-1}) for counterclockwise (resp. clockwise) loops (recall that $Q^{1/2} = q + q^{-1}$). In this representation one can define the spin S_z along the transfer direction (with parallel/antiparallel loops contributing $\pm 1/2$) which acts as a conserved quantum number. Note that $S_z = l$ means that there are at least l non-contractible loops, i.e., loops that wind around the periodic (N) direction of the lattice. Indeed, the contractible loops do not contribute to S_z .

The weights $q^{\pm 1}$ can be further redistributed locally, as a factor of $q^{\alpha/2\pi}$ for a counterclockwise turn through an angle α [7]. While this redistribution correctly weighs contractible loops, the non-contractible loops are given weight 2, but this can be corrected [3] by twisting the model, i.e., by inserting the operator q^{2S_z} into the trace that

⁵Note that we do not factorize $Q^{V/2}$, in order to recover exactly the same expression for the $K_{1,2l+1}$ as before.

defines the partition function. A partial resummation over the oriented-loop splittings at vertices which are compatible with a given orientation of the edges incident to that vertex now gives a six-vertex model representation [7]. Each edge of the medial lattice then carries an arrow, and these arrows are conserved at the vertices: the net arrow flux defines S_z as before. The six-vertex model again needs twisting by the operator q^{S_z} to ensure the correct weighting. Considering each arrow as a spin 1/2, the transfer matrix in the six-vertex representation, T_{6V} , acts on a quantum chain of $2L$ spins 1/2. T_{6V} can be expressed in terms of generators of a Temperley-Lieb algebra, and therefore commutes with the generators of the quantum group $U_q(sl(2))$ [3]. In addition to S_z one can then define the total spin S (corresponding to the Casimir).

In this subsection we now follow [3] and define $K_{1,2l+1}$ as the trace of $(T_{6V})^N$ in the space of highest weights of spin $S = S_z = l$.⁶ With this definition, our goal is to decompose $K_{1,2l+1}$ in terms of the Z_{2j+1} , obtaining again Eq. (12), from which we shall conclude that the two definitions of $K_{1,2l+1}$ are equivalent.

To this end, we first remark that

$$K_{1,2l+1} = F_{2l+1} - F_{2(l+1)+1}, \quad (18)$$

where F_{2l+1} is the trace of $(T_{6V})^N$ on the space of *all* states of spin $S_z = l$. Indeed, the number of highest weight states of spin $S = S_z = l$ equals the number of states of spin $S_z = l$ minus the number of states of spin $S_z = l+1$. Therefore, we first decompose F_{2l+1} . The advantage of working with F_{2l+1} is that only S_z is specified, not S . Indeed, only S_z has a simple interpretation in the oriented loop representation: a basis of the space corresponding to $S_z = l$ is given simply by all states with a net arrow flux of l to the right, whereas the states with $S = S_z = l$ would be more complicated linear combinations of given spin configurations.

We now consider a configuration of oriented loops contributing to Z_{2j+1} , i.e., with $2j$ non-contractible loops. As the contractible loops do not contribute to S_z , there are no constraints on their orientations. Among the $2j$ non-contractible loops, $j+l$ (resp. $j-l$) must be oriented to the right (resp. left) in order to obtain $S_z = l$ (recall that

⁶Note that in this context, Eq. (10) follows by noting that each irreducible representation contains $2l+1$ states, which is replaced by the q -deformed number $(2l+1)_q$ on account of the twist.

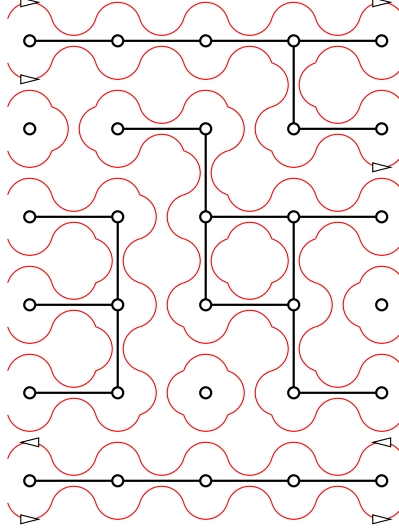


Figure 3: Loop configuration corresponding to the cluster configuration in Fig. 2. The contractible loops can have any orientation (not shown), whereas those of the non-contractible loops are constrained by the chosen value of S_z . With $2j = 4$ non-contractible loops we show one of the four possible orientations leading to $S_z = 1$.

$l \leq j$). This is illustrated in Fig. 3. There are therefore $\binom{2j}{j-l}$ possible orientations of the non-contractible loops compatible with the chosen value of S_z . Correcting for the factors of Q as before, we conclude that the character decomposition of F_{2l+1} is

$$F_{2l+1} = \sum_{j=l}^L \binom{2j}{j-l} \frac{Z_{2j+1}}{Q^j}. \quad (19)$$

Using now Eq. (18), and keeping in mind the identity in Eq. (6), we finally obtain Eq. (12). This proves that our definition of $K_{1,2l+1}$ coincides with the one used in [3].

3.4 Case of p integer

When p is integer, $U_q(sl(2))$ mixes representations with $l' = p - 1 - l + np$ and $l' = l + np$, with n integer. Of particular interest are the type II representations, and it can be shown that the traces on highest weight states of type II are given by [3]

$$\chi_{1,2l+1}(L, N, x) = \sum_{n \geq 0} \left(K_{1,2(np+l)+1}(L, N, x) - K_{1,2((n+1)p-1-l)+1}(L, N, x) \right). \quad (20)$$

For convenience in writing Eq. (20) we have defined $K_{1,2l+1}(L, N, x) \equiv 0$ for $l > L$. At the ferromagnetic critical point, and in the continuum limit, the quantities $\chi_{1,2l+1}$

become characters corresponding to primary fields of the unitary, minimal model $M_{p,p-1}$ with central charge $c = 1 - \frac{6}{p(p-1)}$. The many cancellations in Eq. (20) are linked to the existence of null vectors in the corresponding irreducible Verma modules. In fact, Eq. (20) is then nothing else than the Rocha-Caridi equation [8].

As in the case of the generic characters $K_{1,2l+1}$, the definition (20) of the minimal characters $\chi_{1,2l+1}$ is at finite size, and for any temperature x , but by analogy we shall still refer to $\chi_{1,2l+1}(L, N, x)$ as a minimal character.

It does not appear to be possible to compute the $\chi_{1,2l+1}$ directly in the cluster representation, i.e., otherwise than by first computing the corresponding $K_{1,2l'+1}$ and then applying Eq. (20). They can however be computed directly in an A_{p-1} type RSOS model [9] with specific boundary conditions [10].

Many, but not all, character decompositions of partition functions in terms of $K_{1,2l+1}$ turn into character decompositions in terms of $\chi_{1,2l+1}$ for p integer. This is the case for the total partition function, due to the symmetries

$$c^{(l)} = -c^{(p-1+np-l)} = c^{(np+l)}. \quad (21)$$

Therefore, using Eq. (8), one obtains [10]

$$Z = \sum_{l=0}^{\lfloor (p-2)/2 \rfloor} c^{(l)} \chi_{1,2l+1}. \quad (22)$$

Note that the sum contains less terms than before; in fact it is over those minimal characters that would be inside the Kac table at the ferromagnetic critical point [11].

On the other hand, the formula for the Z_{2j+1} , when the number of NTC is fixed to j , cannot in general be expressed in terms of the $\chi_{1,2l+1}$ for p integer. One interesting exception is for $j = 0$ (no NTC allowed) and p even. Using Eq. (15) one obtains

$$Z_1 = \sum_{l=0}^{\lfloor (p-2)/2 \rfloor} (-1)^l \chi_{1,2l+1} \quad (p \text{ even}). \quad (23)$$

This effect of parity in p is present in many other properties of the RSOS models [12].

4 Fixed transverse boundary conditions

Another constrained partition function whose character decomposition would be of interest is that of the Potts model on a cyclic lattice strip with *fixed* boundary conditions on

the upper and lower horizontal row of Potts spins. It turns out to be easier to obtain the decomposition of a slightly modified object, namely the corresponding partition function on the dual lattice, with fixed boundary conditions on the two dual spins each of which lives on an exterior infinite face.

4.1 A modified model on the dual lattice

We consider therefore $\tilde{Z}_{Q_0}(\tilde{x})$, the partition function of the Potts model, defined on the lattice dual to the $L \times N$ cyclic strip considered in the preceding sections, evaluated at the dual temperature $\tilde{x} = 1/x$. For the sake of generality, any dual cluster which contains one (or both) exterior dual vertices has a weight of Q_0 instead of Q . Note that $Q_0 = 1$ corresponds to fixed boundary conditions on the two exterior dual spins. The case $Q_0 = Q$ is equivalent (under duality) to the free transverse boundary conditions considered above; we denote the corresponding dual partition function $\tilde{Z}(\tilde{x})$.

We search the character decomposition of $\frac{Q^{2-F}v^E}{Q_0}\tilde{Z}_{Q_0}(\tilde{x})$, where the prefactor is chosen so as to make the final result simpler. To achieve this goal, one needs first to convert the weights of the dual clusters into weights of direct clusters. Indeed, by duality a direct cluster configuration is in one-to-one correspondence with a dual cluster configuration [7], as shown in Fig. 4. To simplify the notation, we adopt the following convention: a dual cluster is called a *non-trivial cluster* (NTC) if it is non-contractible with respect to the periodic lattice direction, or if it contains one (or both) of the exterior dual spins. With this convention, a dual configuration with $j + 1$ dual NTC corresponds always to a direct configuration with j direct NTC. Note that there is always at least one dual NTC.

Given a cluster configuration, we denote by t the number of direct trivial (contractible) clusters, by \tilde{t} the number of dual trivial clusters, by b the number of direct edges, and by \tilde{b} the number of dual edges. Consider now the weight of a configuration with $j + 1$ dual NTC in $\frac{Q^{2-F}v^E}{Q_0}\tilde{Z}_{Q_0}(\tilde{x})$. For $j \geq 1$ (resp. $j = 0$) this is $\frac{Q^{2-F}v^E}{Q_0}Q_0^2Q^{j-1}Q^{\tilde{t}}\tilde{v}^{\tilde{b}}$ (resp. $\frac{Q^{2-F}v^E}{Q_0}Q_0Q^{\tilde{t}}\tilde{v}^{\tilde{b}}$), since the two exterior dual vertices are contained in two different (resp. the same) dual NTC. We have here denoted the dual parameter $\tilde{v} = Q/v$.

To express these weights in terms of the direct quantities, we recall the fundamental duality relation [7] $Q^{1-F}v^E\tilde{Z}(\tilde{x}) = Z(x)$, valid because the lattice is planar. Translated

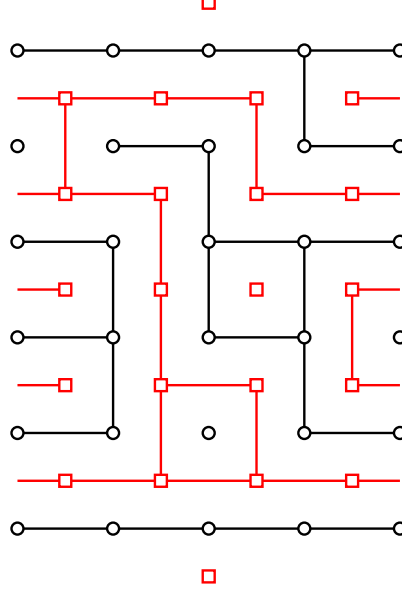


Figure 4: Direct and dual clusters corresponding to the configuration in Fig. 3. Direct (resp. dual) vertices are shown as black circles (resp. red squares). There are two direct NTC and three dual NTC (see text).

into a relation on the weights of a single cluster configuration this reads

$$Q^{1-F} v^E Q^{j+1} Q^{\tilde{t}} \tilde{v}^{\tilde{b}} = Q^j Q^t v^b. \quad (24)$$

Therefore, the weight of a cluster configuration with j direct NTC reads $Q_0 Q^{j-1} Q^t v^b$ if $j \geq 1$, and $Q^t v^b$ if $j = 0$. We thus deduce the following result: the weight of a direct cluster configuration in $\frac{Q^{2-F} v^E}{Q_0} \tilde{Z}_{Q_0}(\tilde{x})$ is the same as in $Z(x)$, except that for $j \geq 1$ direct NTC, one of the NTC has a weight Q_0 instead of Q .

4.2 $\tilde{Z}_{Q_0}(\tilde{x})$ in terms of $K_{1,2l+1}$

Let us recall that when inserting the development (10) of $c^{(l)}$ into Eq. (8) for Z , we have a geometrical interpretation for each term separately: from Eq. (13) the term in Q^j gives precisely Z_{2j+1} . Due to the result given after Eq. (24), we must now simply replace Q^j by $Q_0 Q^{j-1}$ for $j \geq 1$ and keep unchanged the term corresponding to $j = 0$. Therefore

$$\frac{Q^{2-F} v^E}{Q_0} \tilde{Z}_{Q_0}(\tilde{x}) = \sum_{l=0}^L b^{(l)} K_{1,2l+1}(x) \quad (25)$$

with the amplitudes

$$b^{(l)} = \frac{Q_0}{Q} c^{(l)} + (-1)^l \left(1 - \frac{Q_0}{Q}\right) = (-1)^l + \sum_{j=1}^l (-1)^{l-j} \binom{l+j}{l-j} Q_0 Q^{j-1}. \quad (26)$$

Note that when $Q_0 = Q$, we recover $b^{(l)} = c^{(l)}$ as we should.

Just like in the case of free transverse boundary conditions, each power of Q in Eq. (25) can be interpreted separately as a partition function with a fixed number of NTC.

Let us consider a couple of limiting cases of Eq. (25). For $Q_0 \rightarrow 0$, $b^{(l)} = (-1)^l$ and therefore

$$\lim_{Q_0 \rightarrow 0} \left(\frac{Q^{2-F} v^E}{Q_0} \tilde{Z}_{Q_0}(\tilde{x}) \right) = \sum_{l=0}^L (-1)^l K_{1,2l+1}(x) = Z_1(x), \quad (27)$$

where we have used Eq. (15). We thus recover exactly the partition function with no direct NTC.

On the other hand, for $Q_0 \rightarrow \infty$, there is no $K_{1,1}$ in the expansion of $\frac{Q^{2-F} v^E}{Q_0} \tilde{Z}_{Q_0}(\tilde{x})$, i.e., $l = 0$ is forbidden. This is indeed expected, since in that limit there can be no dual cluster connecting the two exterior vertices, and therefore there is at least one direct NTC. Thus $j = 0$ is forbidden, and since $l \geq j$, we deduce that $l = 0$ is forbidden as well.

We now consider the case of p integer. Using Eqs. (26) and (21), we obtain that for p even

$$b^{(l)} = -b^{(p-1+np-l)} = b^{(np+l)}, \quad (28)$$

and we can write

$$\frac{Q^{2-F} v^E}{Q_0} \tilde{Z}_{Q_0}(\tilde{x}) = \sum_{l=0}^{\lfloor (p-2)/2 \rfloor} b^{(l)} \chi_{1,2l+1}(x) \quad (p \text{ even}). \quad (29)$$

Note finally that $b^{(1)} = Q_0 - 1$. This means that with fixed cyclic boundary conditions ($Q_0 = 1$) the term $l = 1$ drops out from the character decomposition. This fact has been exploited in a recent study of partition function zeroes of the RSOS models [13].

4.3 Square lattice model with $Q_0 = 1$

The case of $Q_0 = 1$ can be interpreted in the spin representation as having the same fixed value of the dual spins on the two exterior dual vertices. Alternatively, in the cluster

picture, a dual cluster containing one or both exterior vertices has the weight 1 instead of Q .

Suppose now for simplicity that the direct lattice is a square lattice. The dual lattice is then a square lattice too, except for the two exterior vertices, each of which is equivalent to an extra line of spins all fixed in the same state. To make the equivalence perfect we should include an extra global factor of $\exp(2NJ)$, because of the interactions between spins inside each of the two extra lines (see Fig. 4). The dual lattice is thus equivalent to a square lattice of width $L + 1$ and of length N , with periodic boundary conditions along N and all the spins at the boundaries fixed to the same value. We denote the corresponding partition function $Z_{\text{ff}}(L + 1, N, x)$. Eq. (25) then reads explicitly

$$Z_{\text{ff}}(L, N, x) = \frac{\exp(2NJ)}{Q^{2-F} v^E} \sum_{l=0}^L b^{(l)} K_{1,2l+1}(L - 1, N, \tilde{x}). \quad (30)$$

Let us write out the explicit results for integer Q . For the Ising model ($Q = 2$ or $p = 4$) we have

$$Z_{\text{ff}}(L, N, x) = \frac{\exp(2NJ)}{2^{2-F} v^E} \chi_{1,1}(L - 1, N, \tilde{x}), \quad (31)$$

while for the three-state Potts model ($Q = 3$ or $p = 6$) we find

$$Z_{\text{ff}}(L, N, x) = \frac{\exp(2NJ)}{3^{2-F} v^E} (\chi_{1,1}(L - 1, N, \tilde{x}) + \chi_{1,5}(L - 1, N, \tilde{x})) \quad (32)$$

In the latter case, it is interesting to note that at the ferromagnetic critical point $\chi_{1,1} + \chi_{1,5}$ is nothing but the character of the identity operator with respect to the extended W_3 algebra [14].

5 Conclusion

We have explained in this paper how to decompose various constrained partition functions of the Potts model with cyclic boundary conditions in terms of the characters $K_{1,2l+1}$. These decompositions, whose origin is purely combinatorial, hold true in finite size, for any weakly regular lattice, and at any temperature x .

In particular we can decompose the ratios Z_{2j+1}/Z , which are the probabilities of having exactly j non-trivial clusters. While these probabilities are well-understood in

the continuum limit, at the ferromagnetic critical point at least, our results shed more light on their fine structure, in particular regarding corrections to scaling.

Finally, we have seen that fixed transverse boundary conditions lead to the disappearance of the term with $l = 1$. Physically, one would expect the breaking of the S_Q permutation symmetry of the spin states induced by the fixed boundary conditions to simplify the structure of the complex-temperature phase diagram in the low-temperature phase. This expectation is indeed brought out in a recent numerical study [13].

Acknowledgments.

JLJ thanks the members of the SPhT, where part of this work was done, for their kind hospitality.

References

- [1] P.W. Kasteleyn and C.M. Fortuin, J. Phys. Soc. Jap. Suppl. **26**, 11 (1969); C.M. Fortuin and P.W. Kasteleyn, Physica **57**, 536 (1972).
- [2] J.-F. Richard and J.L. Jacobsen, *Character decomposition of Potts model partition functions. II. Toroidal geometry*, in preparation.
- [3] V. Pasquier and H. Saleur, Nucl. Phys. B **330**, 523–556 (1989).
- [4] S.-C. Chang and R. Shrock, Physica A **347**, 314–352 (2005) [cond-mat/0404524].
- [5] J. Jacobsen and J. Salas J. Stat. Phys. **XXX**, XXX–XXX (2005) [cond-mat/0407444].
- [6] H.W.J. Blöte and M.P. Nightingale, Physica A **112**, 405–465 (1982).
- [7] R. J. Baxter, *Exactly solved models in statistical mechanics* (Academic Press, New York, 1982).
- [8] A. Rocha-Caridi, in S. Lepowski, S. Mandelstam and I.M. Singer (eds.), *Vertex operators in mathematics and physics*, MSRI Publications No. 3 (Springer, New York, 1985), p. 451.

- [9] V. Pasquier, J. Phys. A **20**, L1229 (1987).
- [10] H. Saleur and M. Bauer, Nucl. Phys. B **320**, 591 (1989).
- [11] P. Di Francesco, P. Mathieu and D. S  n  chal, *Conformal field theory* (Springer-Verlag, New York, 1997).
- [12] J.-F. Richard and J.L. Jacobsen, Nucl. Phys. B **731**, 335–351 (2005) [math-ph/0507048].
- [13] J.L. Jacobsen, J.-F. Richard and J. Salas *Complex-temperature phase diagram of Potts and RSOS models*, cond-mat/0511059.
- [14] J. Cardy, Nucl. Phys. B **324**, 581 (1989).